JOURNAL OF CATALYSIS 139, 375–382 (1993)

# Dynamic X-Ray Diffraction Study of an Unreduced Iron Oxide Catalyst in Fischer–Tropsch Synthesis

HEON JUNG AND WILLIAM J. THOMSON

*Department of Chemical Engineering, Washington State University, Pullman, Washington 99164-2710*

Received April 24, 1991; revised September 14, 1992

As a result of a previous *in situ* DXRD study of Fischer–Tropsch synthesis over an unsupported, reduced iron catalyst, a similar study has been undertaken with an unreduced iron oxide catalyst. At 543 K and with $H_2/CO = 3.2$, the initial $\alpha$-$Fe_2O_3$ is immediately reduced to magnetite ($Fe_3O_4$), which is in turn, slowly converted to $\chi$-$Fe_{2.5}C$ via a shrinking core process. Catalytic activity appeared to be directly correlated with the formation of the $\chi$-carbide and it is postulated that this is the catalytically active species. Significantly lower deactivation rates are observed with the unreduced iron catalyst, and it is concluded that this is due to the direct formation of $\chi$-carbide in unreduced iron catalysts, which precludes the $\varepsilon'$-carbide → $\chi$-carbide transformation and avoids the production of the nucleate carbon arising from that transformation. 

## INTRODUCTION

It is known that several forms of iron complexes exist while iron-based catalysts are subjected to Fischer–Tropsch (FT) synthesis. Among them (iron, iron carbides, iron oxide), the role of iron oxide in FT synthesis is still a controversy. For example, Shultz *et al.* proposed a model which hypothesizes that $Fe_3O_4$ has no synthesis activity and the degree of oxidation of iron to magnetite limits the maximum activity of the catalyst (*1*). However, FT synthesis over preoxidized iron foils produced higher yields than that over reduced iron foils (*2*). In addition, several other studies also resulted in higher activity and less deactivation for unreduced vs reduced catalyst (*3–5*). Since, in our previous work with unsupported iron catalysts (*6*), we observed that the decrease in catalyst activity took place simultaneously with the transformation of $\varepsilon'$-carbide to $\chi$-carbide ($2.5\ \varepsilon'$-$Fe_{2.2}C \rightarrow 2.2\ \chi$-$Fe_{2.5}C + 0.3C$), it is interesting to examine the role of this transformation relative to the stability of $Fe_3O_4$ catalysts.

Although there is agreement that the unreduced catalysts (initially in a hematite form) change to a mixture of carbide ($\chi$-$Fe_{2.5}C$) and magnetite ($Fe_3O_4$) during FT synthesis (*3–5*), previous workers are divided in their opinion as to the phase which is responsible for the FT activity. Reymond *et al.* claimed that the magnetite phase was the active catalyst since the increase in the formation of Hägg carbide ($Fe_{2.5}C$) accompanied catalyst deactivation and the decrease of $Fe^{3+}$ and the increase of $Fe^{2+}$ correlated with the increase of activity during the activation period. However, Dictor and Bell reported similar hydrocarbon product distributions for both reduced and unreduced iron oxide, indicating that a common active phase, i.e., Hägg carbide or freshly reduced iron, and not magnetite is the active phase for FT synthesis (*5*). However, the evidence supporting these conclusions is not very conclusive. For example, Reymond *et al.* observed small amounts of carbide formation during the initial activation period. However, they claimed that the carbide phase is not the catalyst since they observed additional quantities of carbide during deactivation. For their claim to be correct, the catalytic activity should have started to decrease as soon as the carbide phase began to form. Furthermore, even though Kuivila et al. (*4*), using Mössbauer spectroscopy, observed



0021-9517/93 $5.00

continuous reduction of bulk $Fe_2O_3$ to $Fe_3O_4$ during the activation period, there was also a small but continuous increase in the carbide phase. Moreover, there are previous reports which clearly show that the activation of reduced iron is associated with the formation of bulk carbide phases (*7–9*).

Iron catalysts usually become deactivated during the course of FT synthesis due to the accumulation of inactive surface carbon (*2, 3, 10*). However, unreduced iron oxide catalysts show strong resistance to deactivation (*3–5*). In fact, the quantity of surface carbon accumulated as a function of reaction time is reported to be consistently less for the unreduced catalyst vs the reduced catalyst (*3*). Since the reason for this difference has not been clearly resolved, an *in situ* dynamic X-ray diffraction (DXRD) study of FT synthesis over unreduced irion oxide was undertaken and is reported here.

The effectiveness of *in situ* DXRD for following gas–solid reaction systems has already been demonstrated for the reduction/oxidation of iron catalysts (*11*), and for carbide formation during FT synthesis over unsupported iron (6). Even though XRD is a bulk measurement technique, the outer surface layers of catalysts can be modified by controlling the degree of reduction or oxidation. For example, during in situ reduction of iron oxide, the reduction can be stopped when small quantities of iron are formed (through XRD monitoring) in order to simulate iron supported on iron oxide. This partially reduced catalyst can in turn be subjected to FT synthesis to compare its catalytic activity (and composition) with that of initially unreduced iron oxide and/or reduced iron catalysts. Since the unreduced iron oxide is known to be more stable to Fischer–Tropsch conditions than freshly reduced iron, experiments such as these can provide insight into the response of unreduced surfaces upon initial exposure to the synthesis gas. These are the procedures that were employed in this work, which was directed toward a determination of the active catalytic phase as well as the deactivation scheme of an unreduced iron oxide FT catalyst.

## EXPERIMENTAL

The catalyst was prepared by drying $Fe(NO_3)_3 \cdot 9H_2O$ (Mallincrodt) in air at 383 K for 48 hr followed by calcining in air at 623 K for 24 hr. The BET area and the pore volume were measured by $N_2$ adsorption (Autosorb 6, Quantachrome) and are 20.3 $m^2/g$ and 0.110 $cm^3/g$, respectively. Gases used in this study were high purity grade and were used after passing through a deoxo unit and then a molecular sieve trap.

The specific details of the DXRD equipment have been given elsewhere (*6, 11*), but it consists of a Siemens D500 $\theta$-$2\theta$ powder diffractometer equipped with a flow-through, Anton–Paar hot stage and a position sensitive detector capable of rapid scanning (60 deg/min) at high resolution (0.01 degrees). Co$K\alpha$ radiation and an iron filter were used in all of the experiments reported here. A thin (less than 0.3 mm) sample of powdered catalyst (particle diameter ~10 $\mu$m) of about 100 mg was placed on a platinum strip which was electrically heated. Gases from the reaction chamber were analyzed by GC as well as continuously by non-dispersive infrared (NDIR) analyzers ($CO_2$ and $CH_4$, Beckman and Horiba, respectively).

The total reduction of the iron oxide ($\alpha$-$Fe_2O_3$ to Fe) was carried out at 543 K in pure flowing hydrogen for 4 hr and the iron particle size was estimated by X-ray line broadening analysis to be 16 nm. After reduction, the sample temperature was adjusted to the desired reaction temperature in flowing hydrogen, followed by a change to the FT synthesis gas mixture once the desired temperature (543 K) was reached (typically, in 20 sec). For experiments with unreduced iron oxides, the catalyst sample was heated from room temperature to 543 K in the flowing (~86 STD ml/min) FT synthesis gas mixture. Reaction runs were carried out at atmospheric pressure, and with a 3.2 $H_2/CO$ gas composition. Under these

conditions, the CO conversion was typically 1% or less. DXRD scans were performed at appropriate time intervals during the run and quantitative analysis of the DXRD data was accomplished by using the "External Standard Method" (*12*) to determine the weight fractions of each phase (iron, iron oxide, and carbide). After a particular reaction period (about 8 hr), pure hydrogen gas was supplied at a flow rate of about 180 STD ml/min, and the temperature was raised to 623 K in 30 sec. During this phase of the experiment, hydrogen "etching" of the catalyst took place and was monitored using both DXRD and gas analyses. Selected experiments were also conducted in a once-through differential packed bed reactor in order to demonstrate that the analysis of catalyst composition by DXRD represented actual behavior. In these experiments, 300 mg of unreduced $\alpha$-$Fe_2O_3$ were heated to 543 K in the FT synthesis gas for a total time-on-stream of 8 hr. Since the packed bed conversions were less than 5% and the DXRD conversions were less than 1%, both types of experiments behave as differential reactors in which heat and mass transfer effects are very small.

## RESULTS AND DISCUSSION

Figure 1 shows the DXRD spectra demonstrating the changes in the composition of the unreduced iron oxide catalyst during FT synthesis at 543 K. Time zero corresponds to the point when the temperature of the catalyst sample, which was in the FT synthesis gas stream ($H_2/CO$ = 3.2), reached 543 K (heating from room temperature to 543 K in 30 sec). As can be seen, $\alpha$-$Fe_2O_3$ (hematite) reduced very rapidly to $Fe_3O_4$ (magnetite), and then $Fe_3O_4$ converted to $\chi$-$Fe_{2.5}C$ slowly. There is no evidence of elemental iron, even after 9 hr on-stream. Separate reduction experiments with both CO (3.2 CO/He) and $H_2$ (0.31 $H_2$/He) at 543 K showed that CO is largely responsible for the reduction of $\alpha$-$Fe_2O_3$ to $Fe_3O_4$. This is corroborated by the fact that the initial formation of $Fe_3O_4$ for the experiment shown in Fig. 1 was accompanied by a large peak of $CO_2$ on the $CO_2$-NDIR. The rate of reduction of hematite to magnetite was higher in the $H_2$/CO mixture than in either CO or $H_2$ at the same partial pressures.

Because of the low conversions, only hydrocarbons up to $C_3$ were produced in sufficient quantities to be measured by gas chromatography. Typical product distributions under quasi-steady-state conditions were: $C_2/C_1 = 0.97$, $C_3/C_1 = 0.05$, $C_2^=/C_2 = 1.37$, and $C_3^=/C_3 \approx 0$. For purposes of monitoring the FT activity, only the $CH_4$ production rate was used as a measure of catalytic activity. Figure 2 shows the weight fractions of each solid-state species and the catalyst activity plotted as a function of the synthesis time. A separate FT synthesis run was also carried out in the differential packed bed reactor to demonstrate that the bulk characterization of the catalyst during *in situ* DXRD represents the actual behavior. As can be seen in Fig. 3, there was very good agreement in terms of the magnitude and time dependency of the reaction rate measured in the DXRD chamber with that measured in the packed bed reactor.

As shown in Fig. 2, the FT synthesis rate increased gradually after the complete reduction of hematite to magnetite and, during this activation period, magnetite gradually converted to $\chi$-$Fe_{2.5}C$. Of course these measurements are bulk measurements and not necessarily representative of a monolayer catalytic surface. For example, high conversions can produce sufficient water to promote the oxidation of both surface carbides and iron to magnetite, generally at conversions above 5% (*13*, *1*). However it appears that surface carbides are not oxidized if particle sizes are small, even at conversions as high as 90% (*14*, *15*) or if reaction temperatures exceed 543 K (*16*). Given the catalytic conditions employed here, oxidation by water is not likely to be a problem and reduced surface species would not be expected to form on top of a carbided surface.

Thus, on the basis of these data, three

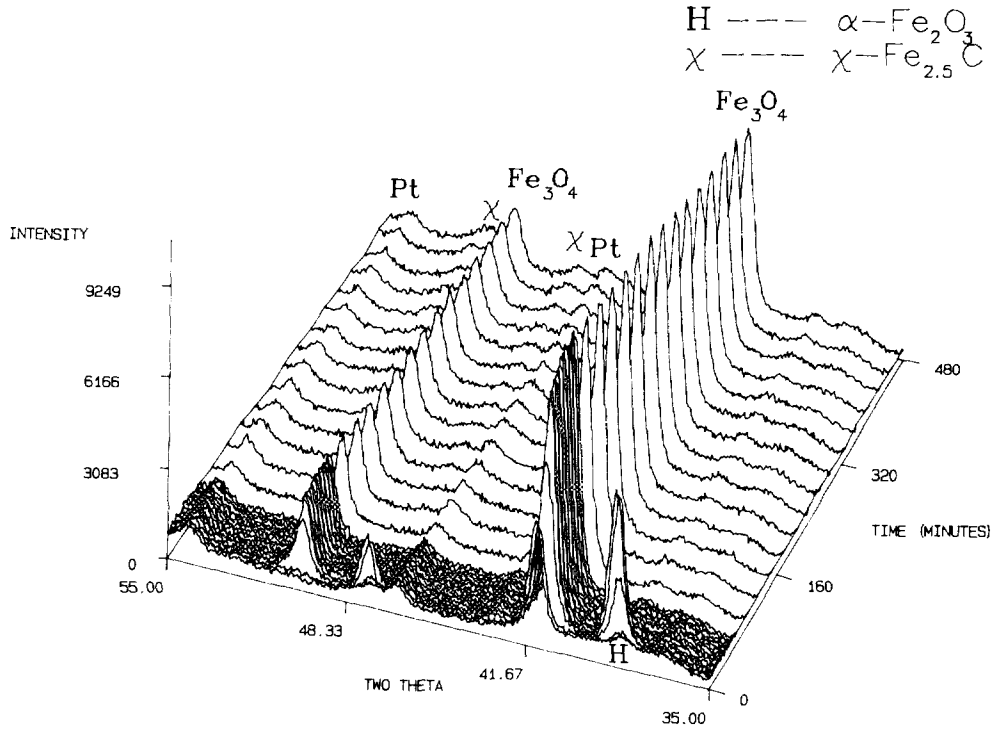


FIG. 1. DXRD data for $\alpha$-$Fe_2O_3$ in FT synthesis at 543 K ($H_2/CO$ = 3.2).

possible catalytically active phases can be postulated: magnetite, freshly reduced iron, or carbide. First of all, the magnetite phase does not seem to play an important role, since FT activity does not correlate with the formation of magnetite. Instead of an immediate increase in activity when the magnetite phase formed, the FT activity gradually increased over the first 6 hr of reaction. The FT synthesis temperature is apparently a factor here. Madon and Taylor (*17*), working with an unsupported, unreduced iron catalyst, observed a rapid reduction in the $CO_2$ product gas when the reaction temperature was raised from 513 to 523 K, suggesting a drastic change in the cata-

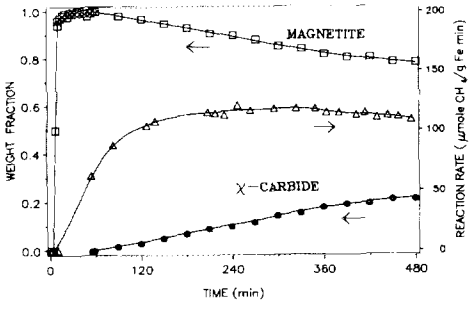


FIG. 2. Catalyst composition and FT activity as a function of synthesis time at 543 K ($H_2/CO$ = 3.2).

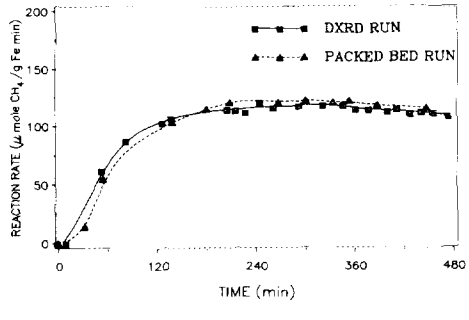


FIG. 3. Comparison of FT activity over $\alpha$-$Fe_2O_3$ in DXRD chamber and that in packed bed reactor ($T$ = 573 K in $H_2/CO$ = 3.2).

lytic surface at the higher temperature. Examination of a spent catalyst which had undergone FT synthesis at 513 K showed only magnetite and no iron or iron carbides. However, when Jacobs (*18*) examined a similar spent catalyst which had been exposed to FT conditions at 533 K, they found $\chi$ and $\varepsilon'$ carbides. Vogler *et al.* (*16*), using $N_2O$ as a probe to measure the oxidation state of surface iron species, also proposed an active surface species which is more reduced than magnetite when magnetite and carbides exist in the bulk. These results are in agreement with our observation that magnetite can be ruled out as the active species when FT synthesis temperatures are at 543 K.

Our simultaneous measurements of both catalyst activity and bulk phase composition during activation show that the gradual activation of the catalyst after $\alpha$-$Fe_2O_3$ was reduced to $Fe_3O_4$ parallels the slow formation of $\chi$-$Fe_{2.5}C$ (Fig. 2). Since elemental iron was not observed by DXRD, it is not clear whether the carbide phase is formed sequentially by the reduction of magnetite to iron and then to the carbide, or by the direct reaction of magnetite with CO. It is clear, however, that if the former case is true, iron is being rapidly converted to the carbide phase as soon as it forms. Since the reduction of magnetite to iron is known to proceed very slowly (*19*), it is more likely that, upon reduction, the iron is immediately converted to the carbide. This explains why iron was never observed in the DXRD experiments. If we postulate that freshly reduced iron is the only active catalyst, then the catalytic activity should drop rapidly once the entire surface has been carbided. Prior to complete carburization, and assuming that the reactant gases can diffuse through the surface carbide layer to reduce magnetite to iron at the carbide/magnetite interface, the catalytic activity should decrease gradually since the interfacial area would decrease as the bulk composition of the carbide increases. Given the behavior of the data in Fig. 2, this hypothesis is not tenable unless iron can be regenerated from the surface carbide by the hydrogen in the mixture gas. However, an *in situ* IR study of CO adsorption on a spent $Fe/Al_2O_3$ catalyst failed to show the CO adsorption bands which would be associated with iron in the metallic state (*20*), indicating that the regeneration of iron does not take place to a measurable extent with these catalysts.

As can be seen in Fig. 2, the increase in catalytic activity accompanies the carbide formation. Despite the fact that this is controversial (*7–10*), the data here are consistent with the carbide phase being the active site for FT synthesis. The fact that the carbide forms only as fast as the reduction of magnetite to iron explains the first stage of activation ($< 60$ min) of the unreduced catalyst. Once the surface has been carburized, the rate of carburization of the remainder of the catalyst is limited by diffusion of the carburizing gases to the carbide/magnetite interface.

During reduction at low temperatures microporosity is created as a result of the increase in the surface area because of the removal of oxygen atoms from the oxide lattice (*21*). When magnetite is converted to $\chi$-$Fe_{25}C$, there also would be the creation of microporosity due to the removal of 1.33 oxygen atoms versus the addition of only 0.4 carbon atoms. Thus, the available carbide surface area would be increased according to the degree of bulk carburization, and this explains the second stage of slow activation (up to 6 hr).

During FT synthesis over iron catalysts, it is known that carbon accumulates on the carbide surface and some of the surface carbon blocks active sites and pores, resulting in deactivation of the catalyst (*2, 3, 10*). This is an explanation for the slow deactivation observed after 6 hr of synthesis. However, the deactivation of the unreduced iron oxide catalyst is significantly slower than that observed in the reduced iron catalyst, as shown in Fig. 4. In order to quantify the surface carbon, the gas stream was changed to pure hydrogen immediately after a DXRD

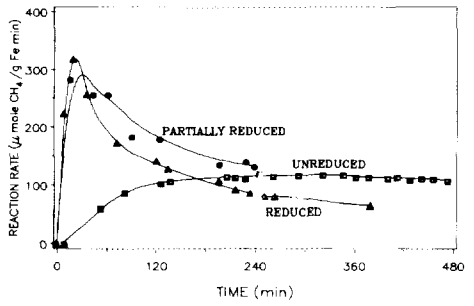


FIG. 4. FT activity as a function of synthesis time for differently treated iron oxides ($T$ = 543 K, $H_2/CO$ = 3.2).

FT synthesis experiment, and the carbon was "etched" from the catalyst. Because the rate of decarburization (carbide → iron) is very slow at 543 K, all of the etching experiments were carried out at 623 K. During the etching experiments, both the change in catalyst composition and the methane evolution were measured by DXRD and $CH_4$-NDIR, respectively. When the total quantity of etched carbon (both the surface carbon and the bulk carbidic carbon) was compared for both catalysts (calculated from the amount of evolved $CH_4$), the carbon etched from the unreduced catalyst was far less than that from the reduced catalysts (C/Fe = 1.00 for unreduced, C/Fe = 2.09 for reduced). Even after accounting for the fact that the reduced iron catalyst was completely converted to carbide in about 10 min of FT synthesis at 543 K (*6*), the surface carbon, $C_s$, etched from the reduced iron catalyst is still far more than that etched from the unreduced catalyst ($C_s$/Fe = 1.69 vs 0.92). In addition, the specific carbide phases formed during carburization of the catalyst were different; only $\chi$-$Fe_{2.5}C$ was formed in the unreduced catalyst whereas a mixture of $\varepsilon'$-$Fe_{2.2}C$ and $\chi$-$Fe_{2.5}C$ was formed in the reduced catalyst (*6, 22*). As stated earlier, based on our previous work, we hypothesized that the carbon from the transformation of $\varepsilon'$-$Fe_{2.2}C$ to $\chi$-$Fe_{2.5}C$ could behave as nucleation sites for further inactive carbon deposition (from the CO reactant), leading to the subsequent deactivation of the reduced catalyst (*6*). This type of deactivation is supported by the work of DeBokx *et al.* (*23*) who demonstrated that carbon filaments grow by the continuous decomposition of metastable carbide intermediates in both Ni and Fe catalysts. Since in this case, $\chi$-$Fe_{2.5}C$ formed directly, the nucleate carbon from the phase transformation is not present, and this alone could account for the increased stability of the unreduced iron catalyst.

It is also interesting to compare our results for unsupported catalysts with previous work on supported iron catalysts. For example, with $Fe/SiO_2$ (*7, 8, 24*) catalysts and with Fe/C catalysts (*25*), only the single $\varepsilon'$-$Fe_{2.2}C$ phase was observed. That is, the $\varepsilon' \rightarrow \chi$ transformation did not occur, even at relatively high temperatures (*7*). The stability of the $\varepsilon'$ phase was attributed to support interactions and, significantly, the activities of the catalysts were very stable. However, when MgO was used as a support (*8, 24*) there were no observable support interactions, $\varepsilon'$ carbide was initially formed and transformed to $\chi$ carbide and deactivation was observed. Thus it appears that the key to a stable iron FT catalyst is to either avoid the formation of $\varepsilon'$ carbide or render it stable if it does form.

Since the data for the unreduced catalyst (Fig. 2) indicate that the catalyst is only 20% carburized, it is likely that deactivation and activation are occurring simultaneously. In other words, even with some degree of deactivation caused by the deposition of inactive carbon, the reactant gases can still diffuse through the surface carbide layer to the carbide/magnetite interface and generate new active sites by carburizing the inside core magnetite. Several experimental observations supports this conclusion, as discussed below.

Figure 5 shows the results of an etching experiment applied to an unreduced catalyst which had been exposed to FT synthesis gas at 543 K for an 8-hr period. At this point there was only 20% carbide and the net de-

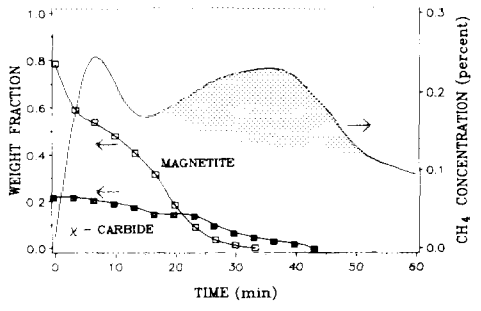


FIG. 5. Catalyst composition and $CH_4$ evolution during $H_2$ etching at 623 K ($\alpha$-$Fe_2O_3$ catalyst exposed to FT synthesis for 8 hr at 543 K, $H_2/CO$ = 3.2); total $CH_4$ evolution (solid line), $CH_4$ from carbidic carbon (shaded area).

activation was very small (see Fig. 2). Upon immediate exposure to $H_2$ at 623 K, the core magnetite was quickly reduced to iron, indicating that $H_2$ had little difficulty diffusing through the outer carbide/carbon layer. Shortly thereafter, the carbide phase began to decarburize and, as can be seen from the total $CH_4$ evolved, surface carbon was etched as well (the shaded area is $CH_4$ from carbidic carbon). Thus it can be concluded that *both* activation (via carbide formation) and deactivation (via surface carbon deposition) are occurring simultaneously.

A qualitative measure of the diffusive nature of the carbide layer can be obtained by observing the "pyrophoric" nature of a spent, carbided catalyst sample. That is, when iron oxide is reduced to iron or magnetite at temperatures below 873 K, it is known to spontaneously oxidize when exposed to air at room temperature (*26*). This is exactly what was observed when, after 8 hr on-stream under FT conditions, an unreduced catalyst was exposed to air at room temperature. This indicates that oxygen can readily diffuse through the carbide layer to react with the inner core of magnetite.

Finally, a separate experiment was also conducted with a partially reduced iron catalyst (~10%) in order to simulate the progressive reduction of magnetite during FT synthesis. Since separate experiments in our laboratory and the published literature (*19, 27*) show that the reduction of iron oxide follows the shrinking core model, the partially reduced iron catalyst has an outside iron layer with an inner magnetite core. When this catalyst was subjected to FT synthesis, iron converted to carbide at a speed similar to that observed with the totally reduced iron catalysts (*6*), and then the magnetite phase slowly converted to carbide in a manner similar to the unreduced catalyst. The change in FT activity of the partially reduced catalyst with time-on-stream is compared for all three catalysts in Fig. 4. As can be seen, the partially reduced catalyst activates much in the same way as the reduced catalyst but deactivates at a rate closer to that observed with the unreduced catalyst. Again, this is consistent with the explanation that the activation of the inner magnetite core for the partially reduced catalyst proceeds at a rate nearly equal to the deactivation of the outer layer.

## CONCLUSIONS

Based on *in situ* DXRD, FT synthesis over an unsupported and unreduced iron oxide, the following conclusions were drawn. The activation of unreduced iron oxide catalysts appears to occur through the formation of $\chi$-$Fe_{2.5}C$ from magnetite, and $\chi$ carbide is believed to be the active catalytic phase for FT synthesis. Activation continues as the inner magnetite core becomes carburized as a result of diffusion of the reactant gases to the magnetite/carbide interface. Significantly lower deactivation rates are observed with the unreduced iron oxide catalyst and are attributed to two factors: the formation of a single stable carbide phase $\chi$-$Fe_{2.5}C$ instead of a mixture of $\varepsilon'$-$Fe_{2.2}C$ and $\chi$-$Fe_{2.5}C$ and the compensating effects of nearly equal activation and deactivation rates. These results are also consistent with the hypothesis that the $\varepsilon' \rightarrow \chi$ carbide transformation generates nucleate carbon which greatly accelerates the deactivation of these catalysts.

ACKNOWLEDGMENT

This material is based on work supported by the National Science Foundation under Grant CBT-8719929. The Government has certain rights in this material.

REFERENCES

1. Schultz, J. F., Hall, W. K., Seligman, B., and Anderson, R. B., *J. Am. Chem. Soc.* **77,** 213 (1955).
2. Dwyer, D. J., and Somorjai, G. A., *J. Catal.* **52,** 291 (1978).
3. Reymond, J. P., Meriaudeau, P., and Teichner, S. J., *J. Catal.* **75,** 39 (1982).
4. Kuivila, C. S., Stair, P. C., and Butt, J. B., *J. Catal.* **118,** 299 (1989).
5. Dictor, R. A., and Bell, A. T., *J. Catal.* **97,** 121 (1986).
6. Jung, H., and Thomson, W. J., *J. Catal.* **134,** 654 (1992).
7. Amelse, J. A., Butt, J. B., and Schwartz, L. H., *J. Phys. Chem.* **82,** 558 (1978).
8. Raupp, G. B. and Delgass, W. N., *J. Catal.* **58,** 361 (1979).
9. Matsumoto, H., *J. Catal.* **86,** 201 (1984).
10. Nimansverdriet, J. W., and van der Kraan, A. M., *J. Catal.* **72,** 385 (1981).
11. Jung, H., and Thomson, W. J., *J. Catal.* **128,** 218 (1991).
12. Cullity, B. D., "Elements of X-Ray Diffraction." Addison–Wesley, Reading, MA, 1978.
13. McCartney, J. T., Hofer, L. J. E., Seligman, B., Lecky, J. A., Peebles, W. C., and Anderson, R. B., *J. Phys. Chem.* **57,** 730 (1953).
14. Satterfield, C. N., Hanlon, R. T., Tung, S.E., Zou, Z., and Papaefthymiou, G. C., *Ind. Eng. Chem. Prod. Res. Dev.* **25,** 401 (1986).
15. Dry, M. E., *Catal. Lett.* **7,** 241 (1990).
16. Vogler, G. L., Jiang, X., Dumesic, J. A., and Maddon, R. J., *J. Catal.* **89,** 116 (1984).
17. Madon, R. J., and Taylor, W. F., *J. Catal.* **69,** 32 (1981).
18. Jacobs, F. E., Ph.D. Dissertation, Princeton Univ., 1980.
19. Colombo, U., Gazzarrini, F., and Lanzavecchia, G., *Mater. Sci. Eng.* **2,** 125 (1967).
20. Perrichon, V., Pijolat, M., and Primet, M., *J. Mol. Catal.* **25,** 207 (1984).
21. Themelis, N. J., and Guavin, W. H., *Trans. Amer. Inst. Min. Metall. Pet. Eng.* **227,** 290 (1960).
22. Niemantsverdriet, J. W., van der Kraan, A. M., van Dijk, and W. L., van der Baan, H. S., *J. Phys. Chem.* **84,** 3363 (1980).
23. De Bokx, P.K., Kock, A. J. H. M., Boellaard, E., Klop, W., and Geus, J. W., *J. Catal.* **96,** 454 (1985).
24. Raupp, G. B., and Delgass, W. N., *J. Catal.* **58,** 348 (1979).
25. Jung, H. J., Vannice, M. A., Mulay, R. M., Stanfield, R.M., and Delgas, W. N., *J. Catal.* **76,** 208 (1982).
26. Turkdogan, E. T., Olsson, R. G., and Vinters, J. V., *Metall. Trans.* **2,** 3189 (1971).
27. McKewan, W. M., *Trans. Amer. Inst. Min. Metall. Pet. Eng.* **218,** 1 (1960).